Multiple Covers with Balls I: Inclusion-Exclusion

Herbert Edelsbrunner, Mabel Iglesias-Ham*

IST Austria (Institute of Science and Technology Austria)
Am Campus 1, 3400 Klosterneuburg, Austria.

Abstract

Inclusion-exclusion is an effective method for computing the volume of a union of measurable sets. We extend it to multiple coverings, proving short inclusion-exclusion formulas for the subset of $\mathbb{R}^n$ covered by at least k balls in a finite set. We implement two of the formulas in dimension $n = 3$ and report on results obtained with our software.

Keywords: Multiple cover with balls, inclusion-exclusion, Voronoi diagrams, hyperplane arrangements, exact computation.

1. Introduction

The work reported in this paper is motivated by configurations of balls that model the organization of DNA inside the nuclei of human cells: the *Spherical* 1 *Mega-base-pairs Chromatin Domain*, or *SCD model*, which is supported by high resolution microscopic observations [1, 2]. It was recently confirmed that inside the chromosome territories in eukaryotic cells, DNA is compartmentalized in sequences of highly interacting segments of roughly the same length [3]. Each segment consists of about one million base pairs which are rolled up in a shape that resembles a round ball, and the shapes are tightly arranged within a restricted space.

Modeling such a configuration as a *packing* – in which the balls are rigid and allowed to touch but not overlap – is too restrictive because the rolled up base pairs push against each other and deform to cover more empty space than is otherwise possible. Similarly, modeling the configuration as a *covering* – in which the balls overlap and cover space without gaps – is not realistic because some empty space is necessary to facilitate the expression and replication of the DNA. We refer to [4] for a representative text in the rich mathematical literature on packings and coverings with balls. For the reason mentioned before, we are motivated to consider configurations that lie between these two extremes: the balls are allowed to overlap and they do not necessarily cover the entire space; see also [5]. Given such a configuration, we are interested in quantifications. For packings and coverings, it is customary to compute the *density*, which is the expected number of balls that contain a random point. This measure can also be used for more general configurations, but there are other choices. To mention one, we may be interested in the set of points each covered by exactly one ball; its volume is the difference between the volume of the union and of the 2-fold cover of the balls. It requires the ability to measure the set of points covered by at least two balls, which is a special case of the question addressed in this paper.

Prior work and results. An effective method for computing the volume of a union of balls, or possibly more general sets, is the principle of inclusion-exclusion. It has a long history in mathematics and is

☆This work is partially supported by the Toposys project FP7-ICT-318493-STREP, and by ESF under the ACAT Research Network Programme.

*Corresponding author

Email addresses: edels@ist.ac.at (Herbert Edelsbrunner), miglesias@ist.ac.at (Mabel Iglesias-Ham)

attributed to Abraham de Moivre (1667–1754) but appeared first in writings of Daniel da Silva (1854) and of James Joseph Sylvester (1883). Given a finite collection of measurable sets, $\mathcal{X}$, in $\mathbb{R}^n$, it asserts that the volume of the union is the alternating sum of the volumes of the common intersections of the sets in all subcollections $Q \subseteq \mathcal{X}$. The formula can be generalized to *k-fold covers*, which we define as the set $\mathbb{X}_k$ of points in $\mathbb{R}^n$ that belong to at least k of the sets:

$$\text{Vol}(\mathbb{X}_k) = \sum_{i \geq k} (-1)^{i-k} \binom{i-1}{k-1} \sum_{Q \in \binom{\mathcal{X}}{i}} \text{Vol}(\bigcap Q); \tag{1}$$

in which $\binom{\mathcal{X}}{i}$ denotes the collection of subsets of size i, see for example Chapter IV of Feller's textbook on probability [6, page 110]. Since we need (1) in the proofs of the short inclusion-exclusion formulas, we give our own proof using the Pascal triangle and its alternating form. If the measurable sets are balls, we write $\mathcal{B}$ for the collection, and $\mathbb{B}_k$ for the k-fold cover. Using the power distance of a point to a ball, the *order-k Voronoi diagram* identifies all collections $Q \subseteq \mathcal{B}$ of size k for which there are points so that the balls in Q are the k closest; see e.g. [7]. Restricting (1) to terms that correspond to cells of the order-k Voronoi diagram, we get a short inclusion-exclusion formula:

$$\text{Vol}(\mathbb{B}_k) = \sum_{\sigma \in \mathcal{V}_k} (-1)^{\text{codim}\, \gamma(\sigma)} \text{Vol}(\bigcap Q_{\gamma(\sigma)}), \tag{2}$$

see the Order-k Pie Theorem in Section 4 for details. Every γ is a cell of the order-k Voronoi diagram, with at least k and at most $k+n$ balls in the corresponding collection $Q_\gamma \subseteq \mathcal{B}$. Relation (2) generalizes the inclusion-exclusion formula of Naiman and Wynn [8] from the union to more general k-fold covers. We also prove a slightly stronger version of (2) in which the sum ranges over the subcollection of cells that have a non-empty common intersection with the balls that define them. It generalizes the inclusion-exclusion formula based on alpha shapes given in [9]. To reduce the size of the terms, we use levels in hyperplane arrangements in $\mathbb{R}^{n+1}$ and inclusion-exclusion formulas for general polyhedra; see [10, 11], and obtain another short inclusion-exclusion formula for the n-dimensional volume of the k-fold cover:

$$\text{Vol}(\mathbb{B}_k) = \sum_{Q \in \mathcal{L}_k} L_Q \cdot \text{Vol}(\bigcap Q); \tag{3}$$

see the Level-k Pie Theorem in Section 5 for details. The collections $Q \subseteq \mathcal{B}$ correspond to affine subspaces of the arrangement, with size between 1 and $n+1$. For $k=1$, the formulas (2) and (3) are the same. Importantly, we have a slightly stronger version of (3) in which all collections of balls are independent. Among other advantages, this additional property eliminates an otherwise necessary case analysis and thus simplifies computer implementations. As mentioned above, the short inclusion-exclusion formulas in (2) and (3) have applications in the study of the spatial organization of chromosomes. We have implemented the formulas in dimension $n=3$, using software supporting exact arithmetic [12, 13] and volume formulas for the common intersection of 3-dimensional balls [14].

Outline. Section 2 extends the principle of inclusion-exclusion from unions to k-fold covers. Section 3 provides background on Voronoi diagrams and hyperplane arrangements. Sections 4 and 5 prove short inclusion-exclusion formulas for k-fold covers with balls in $\mathbb{R}^n$. Section 6 presents results of computational experiments. Section 7 concludes the paper.

2. The Combinatorial Formula

In this section, we explain how the inclusion-exclusion formula for the volume of a union of measurable sets can be extended to k-fold covers. In the context of probability theory, the same extension can be found in [6, page 110]. We begin with a combinatorial result on Pascal triangles.

Recall that the *Pascal triangle* is a 2-dimensional organization of the binomial coefficients, and the *alternating Pascal triangle* is the same except that the coefficients are listed with alternating sign; see

1						
1	1					
1	2	1				
1	3	3	1			
1	4	6	4	1		
1	5	10	10	5	1	
1	6	15	20	15	6	1

1						
-1	1					
1	-2	1				
-1	3	-3	1			
1	-4	6	-4	1		
-1	5	-10	10	-5	1	
1	-6	15	-20	15	-6	1

Figure 1: The first few non-zero rows of the Pascal triangle on the *left*, and of the alternating Pascal triangle on the *right*.

Figure 1. We think of them as (infinitely large) matrices that can be multiplied. To talk about the product, we introduce notation for the u-th row of the Pascal triangle and the v-th column of the alternating Pascal triangle, $R_u, C_v \colon \mathbb{Z} \to \mathbb{Z}$ defined by

$$R_u(v) = \binom{u}{v}, \tag{4}$$

$$C_v(u) = (-1)^{u-v} \binom{u}{v}, \tag{5}$$

where $\binom{u}{v} = 0$ whenever $v < 0$ or $u < v$. In the Pascal triangle, each entry in the u-th row is obtained by adding two entries in the $(u-1)$-st row: $R_u(v) = R_{u-1}(v-1) + R_{u-1}(v)$, unless $u = v = 0$ in which case $R_0(0) = 1$. Similarly, in the alternating Pascal triangle, each entry of the v-th column is obtained by adding two entries in the $(v+1)$-st column: $C_v(u) = C_{v+1}(u) + C_{v+1}(u+1)$, unless $u = v = -1$ in which case $C_{-1}(-1) = 0$. Both rules can be reversed, generating a row from the next row and a column from the previous column:

$$R_{u-1}(v) = \sum_{j \geq 0} (-1)^j R_u(v-j), \tag{6}$$

$$C_{v+1}(u) = \sum_{j \geq 0} (-1)^j C_v(u-j-1). \tag{7}$$

It is easy to prove both relations by induction, but note that (6) requires $u \neq 0$ or $v < 0$ and (7) requires $v \neq -1$ or $u < 0$. Observe that the rows of the Pascal triangle are symmetric: $R_u(v) = R_u(u-v)$ for all u and v. Accordingly, we can reverse the direction of the summation in (6), while the same cannot be done in (7).

Shifted multiplication. As usual in matrix multiplication, we define the product as the matrix whose entry in row u and column v is the scalar product of the u-th row on the left and the v-th column on the right. More generally, we introduce a *shift parameter*, $d \in \mathbb{Z}$, and define

$$M_d(u,v) = \sum_{j=-\infty}^{\infty} R_{u+d}(j) \cdot C_v(j-d). \tag{8}$$

For $d = 0$, this is the usual matrix product, and more generally, it is the product in which the rows of the first matrix are shifted up by d positions and the rows of the second matrix are shifted down by d positions. To get a feeling for the shifted matrix product, we fix a row u_0 in the left matrix and compute scalar products with shifted versions of all columns in the right matrix:

$$N_{u_0}(u,v) = \sum_{j=-\infty}^{\infty} R_{u_0}(j) \cdot C_v(j-u_0+u); \tag{9}$$

see Figure 2 which shows the result for $u_0 = 4$. Note that row R_{u_0} has $u_0 + 1$ non-zero elements which implies that the first non-zero row of N_{u_0} is obtained with shift parameter u_0. More generally, row u is obtained with $d = u_0 - u$, implying that N_{u_0} shares row $u_0 - d$ with M_d. We are particularly interested in row $u_0 - 1$, which N_{u_0} shares with M_1. It is obtained by multiplying row u_0 with all columns shifted down by 1 position.

$$\begin{array}{ccccccc}
1 & & & & & & \\
3 & 1 & & & & & \\
3 & 2 & 1 & & & & \\
1 & 1 & 1 & 1 & & & \\
 & & & & 1 & & \\
 & & & & -1 & 1 & \\
 & & & & 1 & -2 & 1
\end{array}$$

Figure 2: The first few non-zero rows of the matrix N_4.

Lemma 1 (Shift Lemma)**.** *With a shift by $d = 1$ position, we have*

$$M_1(u, v) = \begin{cases} 1 & \text{if } 0 \le v \le u, \\ 0 & \text{otherwise,} \end{cases} \tag{10}$$

for all u and v.

Proof. We note that row u of M_1 is equal to row u of N_{u+1}. It thus suffices to show that

$$N_{u_0}(u, v) = \begin{cases} 1 & \text{if } 0 \le v \le u, \\ 0 & \text{otherwise,} \end{cases} \tag{11}$$

for $u_0 = u + 1$. To see this, we construct the columns of N_{u_0} from left to right. Column 0 is obtained by multiplying R_{u_0} with shifted copies of C_0. Writing $d = u_0 - u$, we get

$$N_{u_0}(u, 0) = \sum_{j=-\infty}^{\infty} R_{u_0}(j) \cdot C_0(j - d) \tag{12}$$

$$= \sum_{j \ge d} (-1)^{j-d} R_{u_0}(j) \tag{13}$$

$$= \sum_{j \ge 0} (-1)^{j} R_{u_0}(d + j) \tag{14}$$

$$= \sum_{j \ge 0} (-1)^{j} R_{u_0}(u - j). \tag{15}$$

We get (13) because the non-zero entries of C_0 alternate between 1 and -1, we get (14) with an index transformation, and we get (15) using $R_{u_0}(v) = R_{u_0}(u_0 - v)$. Note that (15) is the same as the right hand side of (6) after substituting u_0 for u and u for v. We conclude that column 0 of N_{u_0} is the transpose of

R_{u_0-1}. Next we show that column $v+1$ of N_{u_0} can be obtained from column v:

$$N_{u_0}(u, v+1) = \sum_{j=-\infty}^{\infty} R_{u_0}(j) \cdot C_{v+1}(j-d) \tag{16}$$

$$= \sum_{j \geq d+v+1} R_{u_0}(j) \cdot \sum_{i \geq 0} (-1)^i C_v(i') \tag{17}$$

$$= \sum_{i \geq 0} (-1)^i \sum_{j \geq d+v+1} R_{u_0}(j) \cdot C_v(i') \tag{18}$$

$$= \sum_{i \geq 0} (-1)^i N_{u_0}(u-i-1, v), \tag{19}$$

where $i' = j - d - i - 1$. We get (17) using (7), we get (18) by exchanging sums, and we get (19) using (9) and noting that $j - u_0 + (u - i - 1) = i'$. Observe that (19) is but a rewriting of (7) for the columns of N_{u_0}. Applying (19) to column 0, which is R_{u_0-1} transposed, thus gives R_{u_0-2} transposed and shifted down by one position. Repeating the argument, we get transposed copies of R_{u_0-1} down to R_0, progressively shifting down so that their respective last non-zero entries populate row $u_0 - 1$ of N_{u_0}. We thus have $N_{u_0}(u_0 - 1, v) = 1$ for $0 \leq v \leq u_0 - 1$, while the other entries in this row are trivially 0. This implies (11) and therefore the claimed relation. □

Long inclusion-exclusion. We use the insight gained into the Pascal triangles to generalize the principle of inclusion-exclusion from unions to k-fold covers. To make this precise, let $\mathcal{X}$ be a finite collection of sets in $\mathbb{R}^n$. Let k be an integer, and write $\mathbb{X}_k$ for the set of points contained in k or more of the sets in $\mathcal{X}$. We write $\mathbb{X} = \mathbb{X}_1$. Standard inclusion-exclusion implies that the indicator function of the union is the alternating sum of the indicator functions of the common intersections:

$$\mathbf{1}_{\mathbb{X}}(x) = \sum_{i=1}^{\infty} (-1)^{i-1} \sum_{Q \in \binom{\mathcal{X}}{i}} \mathbf{1}_{\bigcap Q}(x). \tag{20}$$

To generalize (20) to k-fold covers, we introduce integer coefficients that depend on the size of the subcollections.

Theorem 1 (k-fold Pie Theorem)**.** *Let $\mathcal{X}$ be a finite collection of measurable sets in $\mathbb{R}^n$, and k a positive integer. Then*

$$\mathrm{Vol}(\mathbb{X}_k) = \sum_{i=k}^{\infty} (-1)^{i-k} \binom{i-1}{k-1} \sum_{Q \in \binom{\mathcal{X}}{i}} \mathrm{Vol}(\bigcap Q). \tag{21}$$

Proof. We prove that the indicator function of the k-fold cover satisfies

$$\mathbf{1}_{\mathbb{X}_k}(x) = \sum_{i=k}^{\infty} (-1)^{i-k} \binom{i-1}{k-1} \sum_{Q \in \binom{\mathcal{X}}{i}} \mathbf{1}_{\bigcap Q}(x). \tag{22}$$

The claimed volume formula follows by integration. Let x be a point in $\mathbb{R}^n$, and let ℓ be the number of sets in $\mathcal{X}$ that contain x. Then x belongs to $\binom{\ell}{i}$ common intersections of i sets, for every $i \geq 1$. Each such common intersection is counted $(-1)^{i-k}\binom{i-1}{k-1} = C_{k-1}(i-1)$ times in (22). Hence, x is counted

$$\binom{\ell}{i} (-1)^{i-k} \binom{i-1}{k-1} = R_\ell(i) \cdot C_{k-1}(i-1) \tag{23}$$

times as a member of the common intersection of i sets. To have a correct indicator function, we need x to be counted once if $1 \leq k \leq \ell$ and zero times otherwise. Indeed,

$$\sum_{i=-\infty}^{\infty} R_\ell(i) \cdot C_{k-1}(i-1) = M_1(\ell-1, k-1), \tag{24}$$

which by the Shift Lemma is 1 if $1 \leq k \leq \ell$ and 0 otherwise, as required. □

3. Geometric Background

This section provides background on Voronoi diagrams and hyperplane arrangements; see de Berg, van Kreveld, Overmars and Schwarzkopf [15] for computational aspects of these concepts.

Covers. Let $B(x, r)$ be the closed ball with center $x \in \mathbb{R}^n$ and radius $r \geq 0$. Writing $B_i = B(x_i, r_i)$, we let $\mathcal{B} = \{B_1, B_2, \ldots, B_m\}$ be a finite set of balls in $\mathbb{R}^n$. For each point $x \in \mathbb{R}^n$, let $\#\mathcal{B}(x)$ be the number of balls in $\mathcal{B}$ that contain x. For every integer k, the *k-fold cover* of $\mathcal{B}$ is

$$\mathbb{B}_k = \{x \in \mathbb{R}^n \mid \#\mathcal{B}(x) \geq k\}, \tag{25}$$

the set of points contained in at least k of the balls; see Figure 3. We write $\mathbb{B} = \mathbb{B}_1$ for the union of the balls. Note that $\mathbb{B}_k = \mathbb{R}^n$ for all $k \leq 0$, $\mathbb{B}_{k+1} \subseteq \mathbb{B}_k$ for all integers k, and $\mathbb{B}_k = \emptyset$ for all $k > m$.

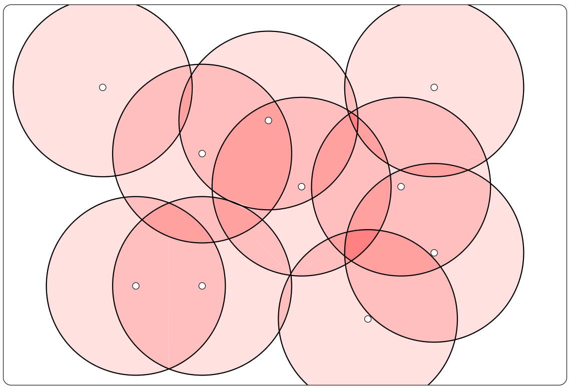

Figure 3: The ten disks have non-empty 1-fold, 2-fold, 3-fold, and 4-fold covers, while the 5-fold cover is empty.

Voronoi diagrams. The *weighted distance* from the ball B_i is defined by the function $\pi_i \colon \mathbb{R}^n \to \mathbb{R}$ that maps a point $x \in \mathbb{R}^n$ to $\pi_i(x) = \|x - x_i\|^2 - r_i^2$. For example if $r_i = 0$, then $\pi_i(x)$ is the squared Euclidean distance from the center of B_i. Following [7], we define the *Voronoi domain* of a subset $Q \subseteq \mathcal{B}$ as the set of points $x \in \mathbb{R}^n$ for which $\pi_q(x) \leq \pi_\ell(x)$ for all $B_q \in Q$ and all $B_\ell \in \mathcal{B} \setminus Q$. Given an integer k, the *order-k Voronoi diagram* of $\mathcal{B}$ is the collection of Voronoi domains of sets Q of size k. As an example, the solid edges in Figure 4 show the order-2 Voronoi diagram of the disks in Figure 3. We find it convenient to generalize the concept by allowing for two parameters, $j < k$. The *Voronoi domain of a pair* $P \subset Q \subseteq \mathcal{B}$ is the set of points x whose weighted distance to the balls in Q is at least that to the balls in P and at most that to the other balls in $\mathcal{B}$:

$$\text{Vor}(P, Q) = \{x \in \mathbb{R}^n \mid \pi_p(x) \leq \pi_q(x) \leq \pi_\ell(x)\}, \tag{26}$$

for all $B_p \in P$, all $B_q \in Q \setminus P$, and all $B_\ell \in \mathcal{B} \setminus Q$. Note that $\text{Vor}(Q) = \text{Vor}(\emptyset, Q)$ is the Voronoi domain of Q as defined above. Being the intersection of finitely many closed half-spaces, $\text{Vor}(P, Q)$ is a possibly empty convex polyhedron. Collecting all Voronoi domains for pairs of sizes $j < k$, we get the (j, k)-*Voronoi diagram*:

$$V_{j,k}(\mathcal{B}) = \{\text{Vor}(P, Q) \mid P \subset Q \subseteq \mathcal{B}\}, \tag{27}$$

where $\operatorname{card} P = j$ and $\operatorname{card} Q = k$; see Figure 4. We are primarily interested in the case $j = 0$, which is the order-k Voronoi diagram, and the case $j = k - 1$, which is the degree-k Voronoi diagram as defined in [16, page 207]. We write $V_k(\mathcal{B}) = V_{0,k}(\mathcal{B})$ and $V(\mathcal{B}) = V_1(\mathcal{B}) = V_{0,1}(\mathcal{B})$.

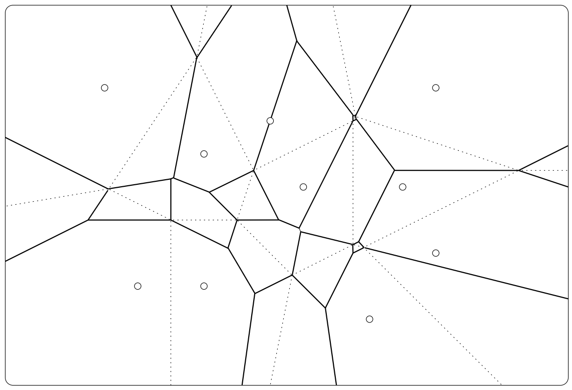

Figure 4: The solid lines show the $(0, 2)$-Voronoi diagram, and the solid together with the dotted lines show the $(1, 2)$-Voronoi diagram of the disks in Figure 3.

A *cell*, γ, of the (j, k)-Voronoi diagram is a non-empty common intersection of a collection of Voronoi domains. We call it an *i-cell* if its dimension is $\dim \gamma = i$ or, equivalently, $\operatorname{codim} \gamma = n - i$. For example, the n-cells are the Voronoi domains, and the 0-cells are the vertices. The cells form a complex in the usual sense of the term: the cells have pairwise disjoint interiors and the boundary of every cell is a union of lower-dimensional cells. As a word of caution, we mention that this complex is not necessarily simple, not even if the balls in $\mathcal{B}$ satisfy reasonable general position requirements. For example, many vertices in the $(1, 2)$-Voronoi diagram shown in Figure 4 belong to six rather than three domains as required for a simple complex in $\mathbb{R}^2$.

Affine functions. Important aspects of the Voronoi diagrams are easier to explain by first mapping the balls in $\mathbb{R}^n$ to non-vertical hyperplanes in $\mathbb{R}^{n+1}$. We therefore introduce the affine functions $A_i \colon \mathbb{R}^n \to \mathbb{R}$ defined by $A_i(x) = 2\langle x, x_i \rangle - \|x_i\|^2 + r_i^2$ for $1 \leq i \leq m$, writing $\mathcal{A} = \mathcal{A}(\mathcal{B})$ for the set of these functions. At each point $x \in \mathbb{R}^n$, we may sort the values of the m functions and form new functions by selecting the pieces where a single function is the k-largest. More formally, we introduce functions $f_k \colon \mathbb{R}^n \to \mathbb{R}$, for $1 \leq k \leq m$, defined by $f_k(x) = \xi$ such that $A_i(x) > \xi$ for at most $k-1$ indices, and $A_i(x) < \xi$ for at most $m-k$ indices. To explain the connection to the Voronoi diagrams of $\mathcal{B}$, we introduce $\varpi \colon \mathbb{R}^n \to \mathbb{R}$ defined by $\varpi(x) = \|x\|^2$. For each $x \in \mathbb{R}^n$, the difference between the values of A_i and ϖ at x is the weighted distance of x from B_i:

$$\varpi(x) - A_i(x) = \|x\|^2 - 2\langle x, x_i \rangle + \|x_i\|^2 - r_i^2 = \|x - x_i\|^2 - r_i^2, \tag{28}$$

for $1 \leq i \leq m$. We can therefore express the k-fold cover as well as the $(k-1, k)$-Voronoi diagram in terms of the arrangement.

Lemma 2 (Level Projection Lemma)**.** *Let $\mathcal{B}$ be a set of m balls in $\mathbb{R}^n$, and $\mathcal{A}$ the corresponding set of affine functions from $\mathbb{R}^n$ to $\mathbb{R}$. Then*

(i) $x \in \mathbb{B}_k$ iff $f_k(x) \geq \varpi(x)$, and
(ii) f_k is affine on every domain of the $(k-1, k)$-Voronoi diagram of $\mathcal{B}$.

Instead of giving a proof, which is not difficult, we illustrate the result in dimension $n = 1$; see Figure 5.

Hyperplane arrangements. The graphs of the A_i are n-planes that partition $\mathbb{R}^{n+1}$ into open convex cells of dimension 0 to $n+1$. We call this partition the *arrangement* of the n-planes. Each *cell* is characterized by a partition $\mathcal{A} = \mathcal{A}^+ \sqcup \mathcal{A}^0 \sqcup \mathcal{A}^-$, and consists of all points $(x, \xi) \in \mathbb{R}^n \times \mathbb{R}$ such that ξ is smaller than, equal

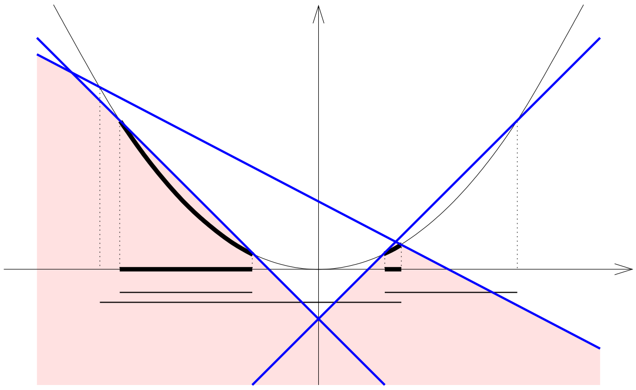

Figure 5: Three intervals in $\mathbb{R}^1$ and the corresponding lines in $\mathbb{R}^2$. The 2-nd level of the arrangement projects to the $(1, 2)$-Voronoi diagram. The points of the parabola that lie on or below the 2-nd level project to the points of the 2-fold cover.

to, larger than $A_i(x)$ whenever $A_i \in \mathcal{A}^+, \mathcal{A}^0, \mathcal{A}^-$. The cells of dimension $n+1$ are referred to as *chambers*. Note that the graph of f_k is a union of cells of dimension 0 to n in the arrangement and does not include any chambers. We call this the *k-th level* of the arrangement. To simplify the exposition, we assume the n-planes are in *general position*. By this we mean that the common intersection of any p of the n-planes in $\mathcal{A}$ is a q-plane with $p+q = n+1$ in $\mathbb{R}^{n+1}$. In particular, if $p > n+1$, then the common intersection is empty. Assuming general position, the subset $\mathcal{A}^0 \subseteq \mathcal{A}$ in the partition that characterizes a q-cell has cardinality p. It follows that the q-cell belongs to exactly p levels of the arrangement.

It is perhaps surprising but not difficult to see that the number of q-cells in an arrangement of m n-planes in general position can be written as a function of m, n, and q and thus does not depend on the n-planes themselves:

$$\#\mathrm{Cells}_q^{n+1}(m) = \binom{m}{p} \cdot \sum_{i=0}^{q} \binom{m-p}{i}, \tag{29}$$

where $p+q = n+1$, as usual; see e.g. [16, page 10]. For example, the number of chambers is $\#\mathrm{Cells}_{n+1}^{n+1}(m) = \sum_{i=0}^{n+1} \binom{m}{i}$. For other values of q, we get the number of q-cells by counting the (q-dimensional) chambers in the arrangements within the q-planes defined by the n-planes. We have $\binom{m}{p}$ such q-planes, with $\#\mathrm{Cells}_q^q(m-p)$ chambers each, which implies (29).

Cubes. In the analysis of local structures within the hyperplane arrangement, we will need a few combinatorial facts about the $(n+1)$-dimensional unit cube, $[0,1]^{n+1}$. For $0 \leq p \leq n+1$, its number of p-faces is

$$\#\mathrm{Faces}_p^{n+1} = \binom{n+1}{p} \cdot 2^{n+1-p}. \tag{30}$$

To see (30), we select $q = n+1-p$ coordinate directions and intersect the $(n+1)$-cube with a q-plane parallel to these directions. There are $\binom{n+1}{q} = \binom{n+1}{p}$ choices, each producing a q-cube with $2^q = 2^{n+1-p}$ vertices. Each of these vertices lies on a p-face of the $(n+1)$-cube.

Each of the $n+1$ coordinates of a vertex u of the $(n+1)$-cube is either 0 or 1, and we write $\#u$ for the number of coordinates that are equal to 1. Directing the edges of the cube from smaller to larger numbers of 1s, we get a partial order of the vertices; see Figure 6. There is a bijection between the faces and the pairs $u \preceq v$ of the partial order, and we call u the *lower* and v the *upper bound* of the face. The dimension of the face is of course $p = \#v - \#u$. As noted in the proof of (30), the p-faces of the $(n+1)$-cube can be organized in $\binom{n+1}{p}$ sets, each the product of a p-face with the vertices of a q-cube. The number of vertices of the q-cube with $\#u = k$ is $\binom{q}{k}$. It follows that the number of p-faces of the $(n+1)$-cube whose lower and

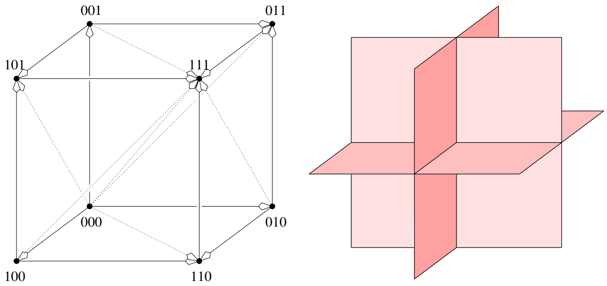

Figure 6: *Left*: the 3-dimensional unit cube with edges indicating the partial order on the vertices. *Right*: the dual vertex star in a 3-dimensional arrangement. The direction we call *vertical downward* in the text is given by the vector from vertex 000 to vertex 111.

upper bounds satisfy $\#u = k$ and $\#v = k + p$ is

$$\#\text{Faces}_{p,k}^{n+1} = \binom{n+1}{p}\binom{q}{k} = \frac{(n+1)!}{p! \cdot k! \cdot (q-k)!}. \tag{31}$$

Note that $\#\text{Faces}_{p,k}^{n+1} = 0$ whenever $p \notin [0, n+1]$ or $k \notin [0, q]$.

4. The Order-k Formulas

In this section, we use the geometry of the problem to derive a first set of short inclusion-exclusion formulas that generalize the formulas in [8, 9] from the union to the k-fold cover.

Star-convexity. As before, we let $\mathcal{B}$ be a finite set of balls in $\mathbb{R}^n$, and we write $\mathbb{B}_k$ for the set of points in $\mathbb{R}^n$ that are contained in at least k of the balls. Writing $V_k = V_{0,k}(\mathcal{B})$ for the order-k Voronoi diagram, we note that its domains decompose the k-fold cover into convex sets; see Figure 7. We need a structural property

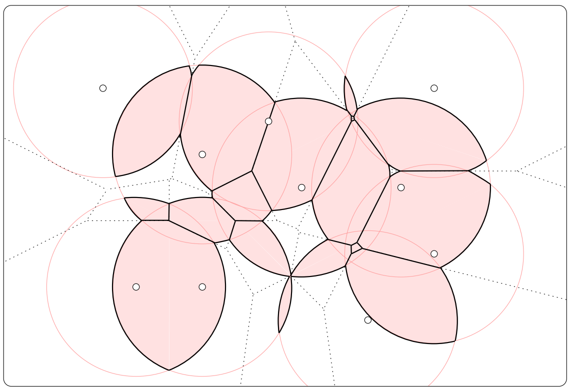

Figure 7: The 2-fold cover of the ten disks in Figure 3. The order-2 Voronoi diagram decomposes the cover into convex sets, each the intersection of a Voronoi domain with two disks.

of the Voronoi domains and their restrictions to the k-fold cover. To state it, we recall that $\text{Vor}(Q)$ is the Voronoi domain of Q, and we write $\text{Res}(Q) = \bigcap Q \cap \text{Vor}(Q)$ for its restriction to the common intersection of the balls. Given a point $x \in \mathbb{R}^n$, we let $\mathcal{Q}_k(x)$ be the system of collections $Q \subseteq \mathcal{B}$ of size k that satisfy $x \in \bigcap Q$ and $\text{Vor}(Q) \neq \emptyset$. Clearly, if $x \notin \mathbb{B}_k$, then $\mathcal{Q}_k(x)$ is empty. If $x \in \mathbb{B}_k$, then $\mathcal{Q}_k(x)$ is necessarily non-empty as it contains all collections Q of size k with $x \in \text{Vor}(Q)$, but there may be additional collections in the system. We are interested in the union of the restricted and unrestricted Voronoi domains whose balls contain the point x:

$$\mathbb{V}_k(x) = \bigcup_{Q \in \mathcal{Q}_k(x)} \mathrm{Vor}(Q), \tag{32}$$

$$\mathbb{R}_k(x) = \bigcup_{Q \in \mathcal{Q}_k(x)} \mathrm{Res}(Q). \tag{33}$$

To prepare the analysis of these sets, we recall a basic property of the weighted distance functions. If B_i and B_j are balls in $\mathbb{R}^n$, then $f\colon \mathbb{R}^n \to \mathbb{R}$ defined by $f(x) = \pi_i(x) - \pi_j(x)$ is an affine function:

$$\begin{aligned} f(x) &= \|x - x_i\|^2 - r_i^2 - \|x - x_j\|^2 + r_j^2 \\ &= 2\langle x, x_j - x_i \rangle + \|x_i\|^2 - \|x_j\|^2 - r_i^2 + r_j^2. \end{aligned} \tag{34}$$

It follows that the restriction of f to any line, L, in $\mathbb{R}^n$ is an affine function that is constant iff L is normal to $x_j - x_i$. The main property of interest is the *star-convexity* of $\mathbb{V}_k(x)$ and $\mathbb{R}_k(x)$. In particular, we will show that for every point y in $\mathbb{V}_k(x)$ or $\mathbb{R}_k(x)$, the entire line segment connecting x with y is contained in this set.

Lemma 3 (Star-convexity Lemma)**.** *Let $\mathcal{B}$ be a finite set of balls in $\mathbb{R}^n$, k an integer, and x a point in $\mathbb{R}^n$. Then $\mathbb{V}_k(x)$ is either empty or star-convex, and so is $\mathbb{R}_k(x)$.*

Proof. We first consider $\mathbb{V}_k(x)$. Assuming $x \in \mathbb{B}_k$, we let y be a point in $\mathbb{V}_k(x)$, and we let Q be a collection of k balls in $\mathcal{B}$ such that $y \in \mathrm{Vor}(Q)$. By construction, the balls in Q minimize the weighted distance for y, and the weighted distance of x to any of these balls is non-positive. Let L be the line that passes through x and y, and let $u \in L$ be strictly between x and y. To derive a contradiction, assume $u \notin \mathbb{V}_k(x)$. Then there exists a ball $B_0 \in \mathcal{B}$ that is among the k closest for u such that $\pi_0(x) > 0$. It can therefore not be in Q. Hence, there is a ball $B_1 \in Q$ with $\pi_0(u) \le \pi_1(u)$. But we also have $\pi_1(y) \le \pi_0(y)$ and $\pi_1(x) < \pi_0(x)$, which contradicts that $\pi_1 - \pi_0$ restricts to an affine function on L. We conclude that $u \in \mathbb{V}_k(x)$, which implies that $\mathbb{V}_k(x)$ is star-convex, as claimed.

The argument for the restricted Voronoi domains is similar, implying that $\mathbb{R}_k(x)$ is star-convex as well. ☐

Short inclusion-exclusion. The formulas we prove have at most one term for each cell in the order-k Voronoi diagram. For constant dimension, the number of such cells is bounded from above by a polynomial in the number of balls, which is much smaller than the number of subsets of the balls. This is our justification for calling the formulas *short*. To state them, we associate each cell γ of V_k with the subset $Q_\gamma \subseteq \mathcal{B}$ of balls that are among the k closest for at least one Voronoi domain containing γ. Assuming general position, we have

$$k \le \mathrm{card}\, Q_\gamma \le k + n. \tag{35}$$

To prove these inequalities, we set $q = n - \dim \gamma$ and observe that $k = \mathrm{card}\, Q_\gamma$ iff $q = 0$. To prove the upper bound, we assume $q > 0$ and let x be an interior point of γ. By assumption of general position, x has equal weighted distance to $q + 1$ balls. Let ℓ be the number of balls to which x has smaller weighted distance than to these $q + 1$ balls. We have $\ell < k$, else γ would not be a face of the Voronoi domains. The k balls defining a Voronoi domain that contains γ include the ℓ balls as well as $k - \ell$ of the $q + 1$ balls. It follows that Q_γ contains the ℓ balls together with the $q + 1$ balls. But $\ell < k$ and $q \le n$, which implies $\mathrm{card}\, Q_\gamma \le \ell + q + 1 \le k + n$, as claimed.

To state the main result of this section, we introduce two subsystems of the nerve of $V_k(\mathcal{B})$, which is an abstract simplicial complex. Recall that every simplex in the nerve is a collection of Voronoi domains that intersect in a non-empty cell of the order-k Voronoi diagram. We call a simplex *maximal* if it is not a proper face of a simplex whose domains intersect in the same cell. The first subsystem, $\mathcal{V}_k$, consists of all maximal simplices in the nerve of $V_k(\mathcal{B})$. Making use of the bijection between the simplices in $\mathcal{V}_k$ and the cells in V_k we write $\gamma(\sigma)$ for the common intersection of the Voronoi domains in $\sigma \in \mathcal{V}_k$. The second subsystem, $\mathcal{R}_k$, is defined similarly, except that it is limited to simplices whose corresponding cells have non-empty intersection with $\mathbb{B}_k$. As before, we pick only maximal simplices from this smaller system.

Theorem 2 (Order-k Pie Theorem)**.** *Let $\mathcal{B}$ be a finite set of balls in $\mathbb{R}^n$, and k an integer. Then the volume of the k-fold cover is*

$$\mathrm{Vol}(\mathbb{B}_k) = \sum_{\sigma \in \mathcal{V}_k} (-1)^{\mathrm{codim}\,\gamma(\sigma)} \mathrm{Vol}(\bigcap Q_{\gamma(\sigma)}), \tag{36}$$

$$= \sum_{\sigma \in \mathcal{R}_k} (-1)^{\mathrm{codim}\,\gamma(\sigma)} \mathrm{Vol}(\bigcap Q_{\gamma(\sigma)}). \tag{37}$$

Proof. We first prove (36). Recall that $\mathbb{V}_k(x)$ is the union of the order-k Voronoi domains, $\mathrm{Vor}(Q)$, such that $x \in \bigcap Q$. Each such domain is a vertex in $\mathcal{V}_k$, and we write $\mathcal{V}_k(x) \subseteq \mathcal{V}_k$ for the simplices these vertices span. We introduce $\chi \colon \mathbb{R}^n \to \mathbb{R}$ defined by mapping x to the Euler characteristic of $\mathbb{V}_k(x)$. To avoid any ambiguity arising for unbounded sets, we clip $\mathbb{R}^n$ to within a sufficiently large n-dimensional box and take the Euler characteristic of $\mathbb{V}_k(x)$ intersected with this box. Recall that $\mathbb{V}_k(x)$ is either empty or star-convex. In the former case, the Euler characteristic is 0, and in the latter case, it is 1. Hence, χ is the indicator function of the k-fold cover:

$$\chi(x) = \begin{cases} 1 & \text{if } x \in \mathbb{B}_k, \\ 0 & \text{if } x \notin \mathbb{B}_k. \end{cases} \tag{38}$$

It follows that $\mathrm{Vol}(\mathbb{B}_k) = \int_{x \in \mathbb{R}^n} \chi(x)\,\mathrm{d}x$. By the Nerve Theorem[17, 18], $\chi(x)$ is the alternating sum of simplices in the nerve of the Voronoi domains whose union is $\mathbb{V}_k(x)$. If the Voronoi diagram is simple, then $\mathcal{V}_k(x)$ contains all and exactly these simplices and we are done. In the general case however, $\mathcal{V}_k(x)$ may contain fewer simplices, and our task is to show that they suffice to compute the Euler characteristic of $\mathbb{V}_k(x)$.

To explain this, let γ be a cell of V_k, and let $\ell + 1 \geq n + 1 - \dim\gamma$ be the number of Voronoi domains that contain γ. The corresponding ℓ-simplex in the nerve of V_k is maximal, but if $\ell + 1 > n + 1 - \dim\gamma$, then this ℓ-simplex has faces that are not maximal. We continue the proof assuming γ is a vertex. Indeed, if $\dim\gamma > 0$ then we may intersect the local configuration with an orthogonal $(n - \dim\gamma)$-plane, which intersects γ in a point. The remainder of the argument would then be worded within this $(n - \dim\gamma)$-dimensional plane.

Thus assuming $\dim\gamma = 0$, we distinguish between the maximal and non-maximal faces by drawing a sufficiently small $(n-1)$-sphere with center at γ. Denote this sphere as S and the n-ball bounded by S as B (Figure 8, left). The Voronoi domains intersect B in $\ell + 1$ cones and S in $\ell + 1$ $(n-1)$-dimensional caps, which are the bases of the cones. The nerve of the cones is isomorphic to the nerve of the Voronoi domains. To relate the nerve of the caps to the nerve of the Voronoi domains, we map each cap in S to the corresponding cone in B. Let τ be a face of the ℓ-simplex, and consider the common intersection of its Voronoi domains. It is not difficult to see that this common intersection is γ iff τ does not correspond to a simplex in the nerve of the caps in S. Since the cones form an n-ball and the $(n-1)$-caps form an $(n-1)$-sphere, the Euler characteristic of their nerves are 1 and $1 + (-1)^{n-1}$, respectively. It follows that the alternating sum of the non-maximal simplices whose Voronoi domains intersect in γ is:

$$1 - (-1)^{\ell} - [1 + (-1^{n-1})] = \begin{cases} 2 & \text{if } \ell \text{ is odd and } n \text{ is even}, \\ 0 & \text{if } \ell - n \text{ is even}, \\ -2 & \text{if } \ell \text{ is even and } n \text{ is odd}. \end{cases} \tag{39}$$

In words, the alternating sum of the non-maximal simplices is precisely the difference between the contribution of the vertex γ and the ℓ-simplex:

$$(-1)^n - (-1)^{\ell} = (-1)^{\mathrm{codim}\,\gamma} - (-1)^{\ell}. \tag{40}$$

This proves the claimed formula for points x equal to or sufficiently close to γ. We need additional arguments for points x that are not contained in the intersection of the k balls for all Voronoi domains meeting at γ.

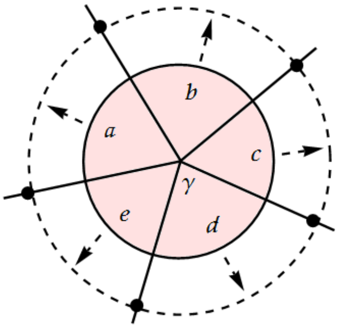

Figure 8: The ℓ-simplex has non-maximal faces $ad, bd, acd, \ldots$. On the left, with $\ell = 4$ and $n = 2$, we shade the ball and draw the partition into caps as dashed arcs. On the right, with $\ell = 4$ and $j = 3$, only a proper subset of the Voronoi domains contain x.

Suppose $j+1 < \ell+1$ of the Voronoi domains meeting at γ contain x in the intersection of their balls. The nerve of the corresponding $j+1$ cones in B is a j-simplex with Euler characteristic equal to 1 (Figure 8, right). We will prove shortly that the Euler characteristic of the corresponding $j+1$ caps is also equal to 1. The alternating sum of the non-maximal faces of the j-simplex is the difference, which vanishes as desired. It remains to prove that the Euler characteristic of the union of the $j+1$ caps is 1. It suffices to prove that this union is homologically trivial, with $\beta_0 = 1$ the only non-zero Betti number. Suppose it is not (Figure 9, left). Then there is a non-bounding cycle, Z, in the union of caps. By construction $Z \subseteq \mathbb{V}_k(x)$, and since $\mathbb{V}_k(x)$ is star-convex we can draw straight line segments from x to all points of Z and thus form a chain, C, with boundary Z (Figure 9, middle). Since we can locally perturb x, we may assume that the point γ does not belong to C. We can therefore centrally project C from γ to S. By construction, the image of this projection is a chain in the union of caps (Figure 9, right). Its boundary is Z, which contradicts the assumption that the union of caps is homologically non-trivial.

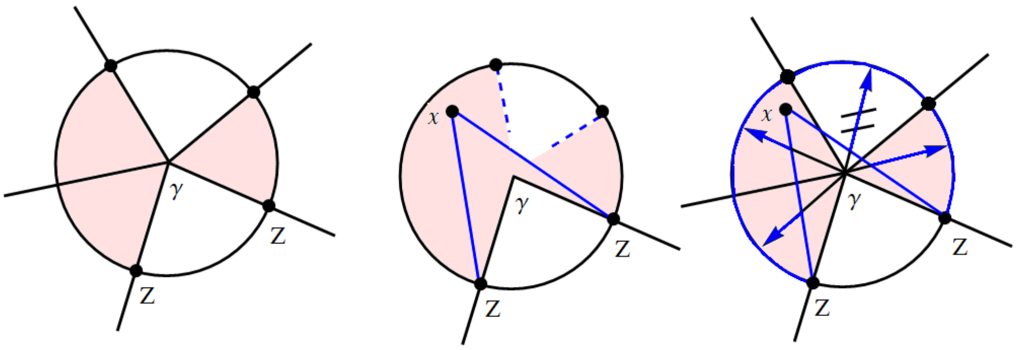

Figure 9: Hypothetical example in which the union of caps is homologically non-trivial, as indicated by the shaded Voronoi domains in $\mathbb{V}_k(x)$. Such configuration leads to a contradiction.

To make the step to the claimed equation, we repackage the contributions of the points x to the integral. Specifically, we focus on a cell γ of the order-k Voronoi diagram. The contribution of γ to the integral is ± 1 times the integral of 1 over all points in $\bigcap Q_\gamma$. The sign alternates with the codimension, which gives $(-1)^{\operatorname{codim} \gamma}$, and the integral evaluates to the volume of the common intersection. This implies (36). The proof of (37) is the same, using again that the sets $\mathbb{R}_k(x)$ are star-convex. □

For $k = 1$, (36) specializes to the formula for the volume of the union of balls given in [8], and (37) specializes to the smaller formula given in [9]. We note that the terms in the difference between the two formulas are not necessarily zero. Even for $k = 1$, the first formula may contain non-zero terms that cancel with others and do not belong to the second formula.

5. The Level-k Formulas

In this section, we present an alternative approach to deriving short inclusion-exclusion formulas for the k-fold cover. Importantly, it leads to formulas whose terms are limited to common intersections of at most $n+1$ balls.

Indicator function for polyhedra. Letting $\mathcal{B}$ be a set of m balls in $\mathbb{R}^n$, we write $\mathcal{A}$ for the corresponding set of m affine functions from $\mathbb{R}^n$ to $\mathbb{R}$, as introduced in Section 2. For an integer k, let $\mathbb{U}_k$ be the set of points $y \in \mathbb{R}^{n+1}$ that lie on or above the k-th level of $\mathcal{A}$, and let $\mathbb{L}_k$ be the set of points on or below the k-th level; see Figure 5, which shows $\mathbb{L}_2$ for three intervals in $\mathbb{R}^1$.

To derive the formulas, we begin with $\mathbb{U}_k$ and then move to $\mathbb{L}_k$. Because $\mathbb{U}_k$ is a not necessarily convex polyhedron, its indicator function can be assembled from simple components, each the indicator function of a face and its immediate neighborhood; see [11]. To explain how this works, we refer to the faces of $\mathbb{U}_k$ as *sides*. For $0 \leq q \leq n$, the q-sides of $\mathbb{U}_k$ are the closures of the q-cells in the arrangement that belong to the k-th level. Clearly, all these cells are convex. The only $(n+1)$-side of $\mathbb{U}_k$ is $\mathbb{U}_k$ itself, which is not necessarily convex but contractible. The *star* of a side, ψ, is the set of sides that contain ψ. Let y be a point in the interior of ψ, and let $\varepsilon > 0$ be small enough such that the sphere, S, with center y and radius ε in $\mathbb{R}^{n+1}$ intersects only sides that belong to the star of ψ. The *negative face figure* of ψ is the union of all half-lines that emanate from y whose central reflections pass through points of the intersection of this sphere with the polyhedron:

$$\mathrm{F}_\psi = \{(1-\lambda)y + \lambda u \mid u \in S \cap \mathbb{U}_k, \lambda \leq 0\}. \tag{41}$$

Intuitively, it is the central reflection of the local view of the polyhedron as seen from y (Figure 10). Note

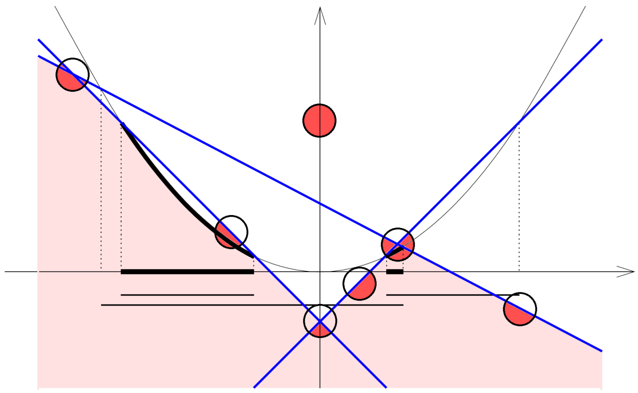

Figure 10: The region $\mathbb{U}_2$ above the second level is white and its complement, $\mathbb{L}_2$, is shaded. For each side ψ of $\mathbb{U}_2$, we draw a sphere centered in the interior of ψ and shade the portion of its inside that points in the direction of its negative face figure.

that F_ψ does not depend on the choice of the point y in the interior of ψ. The main theorem in [11] implies that indicator function of $\mathbb{U}_k$ can be written as an alternating sum of indicator functions of interiors of negative face figures: $\mathbf{1}_{\mathbb{U}_k}(y) = \sum_\psi (-1)^{\mathrm{codim}\,\psi} \cdot \mathbf{1}_{\mathrm{int}\,\mathrm{F}_\psi}(y)$, in which the sum ranges over all sides of $\mathbb{U}_k$, including $\mathbb{U}_k$ itself for which the negative face figure is the entire $\mathbb{R}^{n+1}$. Substituting the closed for the open negative face figures, the indicator function changes from $\mathbb{U}_k$ to $\mathrm{int}\,\mathbb{U}_k$, and subtracting it from 1, it changes to the complement, which is closed:

$$\mathbf{1}_{\mathbb{L}_k}(y) = 1 - \mathbf{1}_{\mathrm{int}\,\mathbb{U}_k}(y) = \sum_\psi (-1)^{n-\dim\psi} \cdot \mathbf{1}_{\mathrm{F}_\psi}(y), \tag{42}$$

in which the sum now ranges over all sides of dimension 0 to n, which are the same for $\mathbb{U}_k$ and $\mathbb{L}_k$.

Negative face figures. To further decompose the indicator function given in (42), we need to understand the negative face figures. It suffices to study a vertex, since the negative face figure of a q-side is that of a vertex in an arrangement of $(n-q)$-planes in $\mathbb{R}^{n+1-q}$, extruded along q additional dimensions. Assuming general position, a vertex w is the intersection of $n+1$ n-planes in $\mathbb{R}^{n+1}$, and its star is dual to a cube of dimension $n+1$; see Figure 6. The n-planes are non-vertical so we can order the chambers accordingly, which corresponds to directing the edges of the cube from top to bottom. To make this concrete, we sort the n-planes, and we assign to each chamber a string of $n+1$ labels in which the p-th label is 0 if the chamber lies above the p-th n-plane, and it is 1 if the chamber lies below the p-th n-plane. It should be clear that the assigned labels are the coordinates of the corresponding vertices of the dual $(n+1)$-cube. Let $k_0 + \ell_0 = m - (n+1)$ such that w lies below k_0 and above ℓ_0 of the n-planes. It follows that w belongs to the k-th level of $\mathcal{A}$ iff $k_0 < k \leq m - \ell_0$. Which cells around w belong to the k-th level and are therefore sides $\mathbb{L}_k$ depends solely on $j = j(w) = k - k_0$, which we call the *index* of w. Specifically, the q-cells that belong to the k-th level are dual to p-faces of the $(n+1)$-cube whose lower and upper bounds satisfy $\#u < j \leq \#v$. Using (31), we see that the number of such q-cells is

$$\#\mathrm{Sides}_{q,j}^{n+1} = \sum_{i=j-p}^{j-1} \#\mathrm{Faces}_{p,i}^{n+1}. \tag{43}$$

Depending on the index of w, different cells in its neighborhood contribute to the indicator function of its negative face figure. For example in 3 dimensions, we have three indicator functions:

$$j = 1 : abc, \tag{44}$$
$$j = 2 : ab + ac + bc - 2abc, \tag{45}$$
$$j = 3 : a + b + c - ab - ac - bc + abc, \tag{46}$$

where we write a, b, c for the indicator functions of the half-spaces bounded from above by the graphs of the three affine functions. In dimension $n+1$, there are $n+1$ indices and $n+1$ different indicator functions of the negative face figures. To express them formally, we write $\mathbf{1}_A$ for the indicator function of the half-space bounded from above by the affine function A.

Lemma 4 (Face Figure Lemma)**.** *Let $\mathcal{A}$ be a set of $n+1$ affine functions from $\mathbb{R}^n$ to $\mathbb{R}$ whose graphs form an arrangement with a single vertex w in $\mathbb{R}^{n+1}$. For $1 \leq j \leq n+1$, the indicator function of the negative face figure of w with index j satisfies*

$$\mathbf{1}_{\mathrm{F}_w}(y) = \sum_{i=n+2-j}^{n+1} (-1)^{i-n+j} \binom{i-1}{n-j+1} \sum_{\mathcal{A}' \in \binom{\mathcal{A}}{i}} \prod_{A \in \mathcal{A}'} \mathbf{1}_A(y). \tag{47}$$

Proof. Since we have only $n+1$ affine functions in $\mathbb{R}^n$, we cannot gain from the geometry of the situation and use the general inclusion-exclusion formula (1). Specifically, we use the indicator function from which (1) follows by integration:

$$\mathbf{1}_{\mathbb{X}_k}(y) = \sum_{i \geq k} (-1)^{i-k} \binom{i-1}{k-1} \sum_{Q \in \binom{\mathcal{X}}{i}} \mathbf{1}_{\bigcap Q}(y), \tag{48}$$

where $\mathcal{X}$ denotes a finite collection of measurable sets in $\mathbb{R}^{n+1}$, and $\mathbb{X}_k$ is the k-fold cover. To specialize this result to our situation, we note that the negative face figure of w is the $(n+2-j)$-fold cover of the $n+1$ closed half-spaces bounded from above by the graphs of the $A_i \in \mathcal{A}$. Substituting $n+2-j$ for k and $\mathcal{A}$ for $\mathcal{X}$, and writing the indicator function of the intersection as a product, we get the claimed relation. ☐

Short inclusion-exclusion. Combining (42) and (47), we get the indicator function of $\mathbb{L}_k$ with terms that are products of at most $n+1$ indicator functions of half-spaces. To state it formally, we write $\mathcal{L}_k$ for the abstract simplicial complex whose abstract simplices are the collections $Q \subseteq \mathcal{B}$ such that the graphs of the corresponding affine functions contain a common side of $\mathbb{L}_k$. For each $Q \in \mathcal{L}_k$, we write $\mathbf{1}_Q \colon \mathbb{R}^{n+1} \to \{0,1\}$ for the indicator function of the intersection of half-spaces bounded from above by the graphs of the corresponding affine functions. Combining the mentioned relations, we get $\mathbf{1}_{\mathbb{L}_k}(y) = \sum_{Q \in \mathcal{L}_k} L_Q \cdot \mathbf{1}_Q(y)$, in which L_Q is sum of coefficients of $\mathbf{1}_Q(y)$ contributed by the various negative face figures. We can now compute the n-dimensional volume of the k-fold cover of the set of balls in $\mathcal{B}$ by integration:

$$\mathrm{Vol}(\mathbb{B}_k) = \int_{x \in \mathbb{R}^n} \mathbf{1}_{\mathbb{L}_k}(x, \|x\|^2)\,\mathrm{d}x = \sum_{Q \in \mathcal{L}_k} L_Q \int_{x \in \mathbb{R}^n} \mathbf{1}_Q(x, \|x\|^2)\,\mathrm{d}x. \tag{49}$$

Note that the last integral is the volume of the intersection of the balls. This gives the first inclusion-exclusion formula for the volume of $\mathbb{B}_k$ derived in this section. However, there are redundant terms that can be removed to obtain an even shorter formula. To identify them, we call a collection of balls, Q, *independent* if for every $P \subseteq Q$ there is a point $x \in \mathbb{R}^n$ such that every ball in P contains x and every ball in $Q \setminus P$ does not contain x; that is: $\bigcap P \setminus \bigcup (Q \setminus P) \neq \emptyset$. Let $\mathcal{I}_k$ be the system of collections $Q \in \mathcal{L}_k$ such that Q is independent. We claim there are integer coefficients I_Q not necessarily equal to L_Q such that the weighted sum over $\mathcal{I}_k$ gives the volume of the k-fold cover. We state both results.

Theorem 3 (Level-k Pie Theorem)**.** *Let $\mathcal{B}$ be a finite set of balls in $\mathbb{R}^n$, and k an integer. Then the volume of the k-fold cover is*

$$\mathrm{Vol}(\mathbb{B}_k) = \sum_{Q \in \mathcal{L}_k} L_Q \cdot \mathrm{Vol}\big(\bigcap Q\big) \tag{50}$$

$$= \sum_{Q \in \mathcal{I}_k} I_Q \cdot \mathrm{Vol}\big(\bigcap Q\big). \tag{51}$$

Proof. The proof of (50) has been given above. To prove (51), we show that whenever $Q \in \mathcal{L}_k$ is not independent, then $\mathrm{Vol}(\bigcap Q)$ can be written as an integer combination of the $\mathrm{Vol}(\bigcap P)$ in which the P are proper subsets of Q. Repeated substitution of dependent terms in (50) eventually gives (51). To prove that the substitution is always possible, we consider the system of linear equations that relates the volumes of the common intersections with the volumes of the cells that appear in the definition of independence. Writing

$$\mu = \Big[\mathrm{Vol}\big(\bigcap P\big)\Big]_{\emptyset \neq P \subseteq Q}, \quad \nu = \Big[\mathrm{Vol}\big(\bigcap P \setminus \bigcup (Q \setminus P)\big)\Big]_{\emptyset \neq P \subseteq Q} \tag{52}$$

for the vectors of volumes, we get $\mu = M\nu$, in which M is a 0-1 matrix. Writing $q = \mathrm{card}\, Q$, M is a $2^q - 1$ times $2^q - 1$ matrix. It has the regular structure reflecting the incidences between the linear spaces spanned by the non-empty subsets of q independent vectors; see Figure 11 for an example. In particular, all entries in the diagonal are 1, and all entries above the diagonal are 0. Furthermore, the number of non-zero entries in each row is a power of 2.

Assume now that Q is not independent. Then at least one component of ν is zero. Equivalently, we may set the corresponding column of M to zero, without violating the correctness of $\mu = M\nu$. This creates dependences between the linear equations. We use the special structure of M to prove that in this case, we can write the volume of $\bigcap Q$ as an integer combination of the $\mathrm{Vol}(\bigcap P)$, in which $P \subseteq Q$ but $P \neq Q$. Fixing $2 \leq r \leq 2^q - 1$, we can reduce the r-th row until its only non-zero entry is in the diagonal of M. To do this, we work from the diagonal element backward, adding an integer multiple of a row above for every non-zero entry. Since $r \geq 2$, the r-th row contains an even number of 1s before reduction. Adding an integer multiple of any row other than the first changes the sum of non-zero entries by an even number, and since the sum in the end is odd, we conclude that the first row has been added with a non-zero coefficient. If we now set the r-th column to zero, we have a zero r-th row. But this implies that the first row is an integer combination of the r-th row and all rows used in its reduction, other than the first row of course. ◻

	uvw	uv	uw	vw	u	v	w
uvw	1						
uv	1	1					
uw	1		1				
vw	1			1			
u	1	1	1		1		
v	1	1		1		1	
w	1		1	1			1

Figure 11: The matrix relating the vectors μ and ν for a collection of size $\text{card}\, Q = 3$.

6. Computation

In this section, we comment on the main challenges in implementing the inclusion-exclusion formulas for the k-fold cover of balls proved in the preceding sections. Our main concern is the correctness of the formulas, leaving considerations of size and speed to future research. We begin with experimental results for a small 3-dimensional example.

Example. As explained shortly, we implemented two formulas in $n = 3$ dimensions: the order-k formula (36) and the level-k formula (50), both after reduction. The reduced formulas are readily evaluated without further case analysis. The input for our example is generated by sampling 10 points uniformly at random from the unit cube in $\mathbb{R}^3$. Centering balls of radius 0.25 at these points gives the first set, $\mathcal{B}_1$, and increasing the radius to 0.875 gives the second set, $\mathcal{B}_2$, see Figure 12.

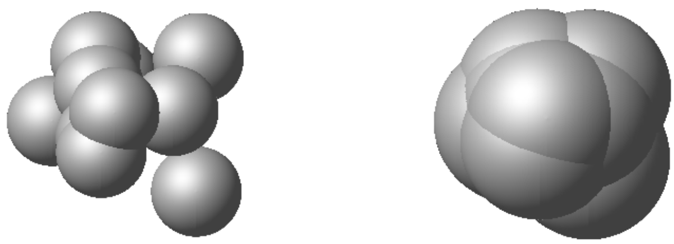

Figure 12: Two sets of ten random balls with centers in the unit cube and radii 0.25 on the *left* and radii 0.875 on the *right*.

Computing the volume of the k-fold cover of $\mathcal{B}_1$ and $\mathcal{B}_2$, for $k = 1, 2, \ldots, 10$, we show the volume as well as the number of terms and the average number of balls per term in Table 1. In every case, the reduced order-k formula is identical to the reduced level-k formula, so we show only three integers per case: the number of terms of the order-k formula (36), of the level-k formula (50), and of the reduced formula. While the number of terms in the level-k formulas tend to be smaller than in the order-k formulas, the difference is neither significant nor consistent. We also note that for $\mathcal{B}_1$, most redundant terms have zero volume, while for $\mathcal{B}_2$, all redundant terms have non-zero volume.

Algorithm. Without going into details, we sketch the main steps in constructing and evaluating an inclusion-exclusion formula for the k-fold cover of a set $\mathcal{B}$ of m balls in $\mathbb{R}^3$. For the order-k formula (36), we construct the order-k Voronoi diagram of $\mathcal{B}$ as the order-1 (weighted) Voronoi diagram of the k-fold averages, as explained in [19]. The latter diagram is then computed with the 3D CGAL weighted Delaunay triangulation software [13]. For the level-k formula (50), we construct in addition the order-$(k-1)$ Voronoi diagram

	$\mathcal{B}_1$, radius = 0.25				$\mathcal{B}_2$, radius = 0.875			
k	order-k	level-k	reduced	vol	order-k	level-k	reduced	vol
1	103 × 2.7	103 × 2.7	34 × 2.0	0.523	103 × 2.7	103 × 2.7	95 × 2.6	7.842
2	166 × 3.4	166 × 3.1	29 × 2.4	0.106	166 × 3.4	166 × 3.1	149 × 3.0	5.176
3	220 × 4.3	219 × 3.4	14 × 2.9	0.023	220 × 4.3	219 × 3.4	186 × 3.4	4.137
4	221 × 5.1	228 × 3.6	4 × 3.3	0.001	221 × 5.1	228 × 3.6	191 × 3.5	3.118
5	190 × 6.0	238 × 3.6	0 × 0.0	0.000	190 × 6.0	238 × 3.6	189 × 3.6	2.450
6					140 × 6.8	203 × 3.7	156 × 3.7	1.857
7					80 × 7.6	184 × 3.6	128 × 3.6	1.417
8					34 × 8.3	127 × 3.5	80 × 3.5	1.024
9					9 × 9.1	65 × 3.4	32 × 3.5	0.704
10					1 × 10.0	17 × 3.3	11 × 3.4	0.332

Table 1: The volume of the k-fold covers of $\mathcal{B}_1$ and $\mathcal{B}_2$, together with the number of terms in the inclusion-exclusion formulas and the average number of balls per term.

and we obtain $V_{k-1,k}(\mathcal{B})$ by superimposing $V_{k-1}(\mathcal{B})$ and $V_k(\mathcal{B})$. While there are standard procedures, we mention that superimposing the two diagrams was perhaps the most laborious task in implementing the algorithm. An important aspect of the above computations is the use of exact arithmetic in making final decisions on the connectivity of the diagrams. Without it, there is little hope to get correct inclusion-exclusion formulas. CGAL offers the exact computation paradigm [20] as part of the package, which is the main reason we decided to use CGAL and not one of the many available alternatives. To illustrate the need for exact arithmetic, we mention that already for $k = 2$, the order-k Voronoi diagram is not simple even if the balls are in general position. Taking $m = 4$ points not in a plane, the order-2 Voronoi diagram has six domains that meet at the center of the circumsphere. This is in contrast to the at most four domains that are allowed to meet in a simple diagram in $\mathbb{R}^3$.

Assuming we have $V_k(\mathcal{B})$ or $V_{k-1,k}(\mathcal{B})$, we construct the formula by translating each cell into a term or a small number of terms. This is straightforward for the order-k formula but can be confusing for the level-k formula, for which we give some more details. Iterating over all cells ψ of $V_{k-1,k}(\mathcal{B})$, we write $j(\psi)$ for its index in the corresponding arrangement, as defined in Section 4. We begin with an initially empty formula.

CASE 1: $\dim \psi = 3$. Add the volume of the corresponding ball to the formula.

CASE 2: $\dim \psi = 2$. Set $i = 3 - j(\psi)$ and subtract the volume of the i-fold cover of the two corresponding balls.

CASE 3: $\dim \psi = 1$. Set $i = 4 - j(\psi)$ and add the volume of the i-fold cover of the three corresponding balls.

CASE 4: $\dim \psi = 0$. Set $i = 5 - j(\psi)$ and subtract the volume of the i-fold cover of the four corresponding balls.

Once we have the complete formula, we evaluate it, translating each i-fold cover to an alternating sum of intersections among the balls. But even this is not an easy task as the balls we intersect are not in any particular geometric configuration. We therefore first reduce the formula until all terms are independent, as explained shortly. In the reduced formula, we have only four different cases: one, two, three, and four independent balls. Analytic formulas for computing the volume of the intersection in each case can be found in [14].

Reduction. Assume we have an inclusion-exclusion formula for the volume of the k-fold cover of m balls in $\mathbb{R}^3$. Each term is a common intersection of balls, but the collections are not necessarily independent. We now explain how to reduce this formula into a form in which all collections are independent. We proceed one term at a time, starting with one whose collection has a maximum number of balls.

Let Q be the balls that appear in the considered term, and write $q + 1 = \operatorname{card} Q$. If $q > 3$, then we can be sure that Q is not independent, and we can replace this term using a relation computed as described in the proof of the Level-k Pie Theorem. To get started, we need a subset P of Q whose common intersection is contained in the union of $Q \setminus P$, and to find it, we use the affine functions from $\mathbb{R}^3 \to \mathbb{R}$, writing A_i for the ones that correspond to balls in P, and A_j for the ones that correspond to balls in $Q \setminus P$. A point $x \in \mathbb{R}^3$ belongs to $\bigcap P$ iff $\|x\|^2 \leq A_i(x)$ for all A_i, and x does not belong to $\bigcup(Q \setminus P)$ iff $\|x\|^2 > A_j(x)$ for all A_j. Hence, for $\bigcap P \setminus \bigcup(Q \setminus P)$ to be non-empty, it is necessary that the chamber below the hyperplanes defined by the A_i and above the hyperplanes defined by the A_j exists. Recalling the formula for the number of chambers in $n+1=4$ dimensions (29), we see that for $q+1>4$ hyperplanes their number is less than 2^{q+1}. It follows that there is at least one subset P whose corresponding chamber is empty. This subset witnesses the non-independence of Q and can be used to start the procedure outlined in the proof of the Level-k Pie Theorem. A drawback of this procedure is the exponential size of the matrix, but it suffices to run it on a subset $Q' \subseteq Q$ of $5 \leq q+1$ balls, and to use the relation for Q' to get a relation for Q.

The above method for finding P does not work for sets Q with cardinality $q+1 \leq 4$. But here we can use the fact that Q is independent iff the nerve of the Voronoi domains restricted to the balls is the full q-simplex spanned by the centers of the $q+1$ balls. If Q is not independent, then the simplices missing from the nerve give the desired relation. To see this, we note that the full q-simplex and the mentioned nerve give two different inclusion-exclusion formulas for the union of the $q+1$ balls [9]. The difference of the two evaluates to zero and contains the intersection of the $q+1$ balls as a term.

7. Discussion

The main results of this paper are short inclusion-exclusion formulas for the k-fold cover of a finite set of balls in $\mathbb{R}^n$, one based on the order-k Voronoi (or power) diagram, and the other on the k-th level in the lifted hyperplane arrangement. In addition, we have formalized the reduction to independent terms, which is essential to get effective implementations of the formulas. This work raises a number of questions we have not been able to answer.

- How big are the formulas, in terms of k, m, n, and how fast can they be computed? For constant dimension, the level-k formula gives a polynomial upper bound, but we do not know an asymptotically tight bound.

The same claim is probably not true for the order-k formula for which the reduction may take a large number of steps. Another advantage of the level-k approach is it extends to computing the volume of weighted multiple covers: assigning a real weight to every ball, we ask for the volume of the set of points covered by balls whose sum of weights exceeds a given threshold. What about shapes that are more general than balls?

- Following a general reduction argument, we see that families of simple shapes, such as ellipsoids and axes-aligned boxes, also have short inclusion-exclusion formulas for the k-fold cover. Are there polynomial-time methods to compute them?

Indeed, it is not difficult to generalize the reduction outlined in the proof of the Level-k Pie Theorem to shapes for which the cardinality of an independent collection is bounded. Starting from the exponential size formula (1), we can reduce the terms until they are all independent, but this approach takes exponential time. Finally, there is the less specific connection of the work in this paper to optimal sphere arrangements that neither pack nor cover. We mention one such question:

- What is the best way to arrange equal-size balls in $\mathbb{R}^n$ if the objective is to maximize the probability that a random point is covered by exactly one ball?

Based on the application of our work and software to the SDC model of the eukaryotic cell nucleus, we hope to identify additional promising optimization criteria.

References

[1] T. Cremer, G. Kreth, H. Koester, R. H. A. Fink, R. Heintzmann, M. Cremer, I. Solovei, D. Zink, C. Cremer, Chromosome territories, interchromatin domain compartment, and nuclear matrix: An integrated view of the functional nuclear architecture, *Critical Reviews in Eukaryotic Gene Expression* **10** (2) (2000) 179–212.

[2] G. Kreth, P. Edelmann, C. Cremer, Towards a dynamical approach for the simulation of large scale, cancer correlated chromatin structures, *Supplement of Italian Journal of Anatomy and Embryology* **106** (2 Suppl 1) (2001) 21–30.

[3] J. Dixon, S. Selvaraj, F. Yue, A. Kim, Y. Li, Y. Shen, M. Hu, J. Liu, B. Ren, Topological domains in mammalian genomes identified by analysis of chromatin interactions, *Nature* **485** (5) (2012) 376–380.

[4] J. H. Conway, N. J. A. Sloane, E. Bannai, *Sphere-packings, Lattices, and Groups*, Springer-Verlag New York, Inc., New York, NY, USA, 1987.

[5] A. Schürmann, F. Vallentin, Computational approaches to lattice packing and covering problems, *Discrete & Computational Geometry* **35** (1) (2006) 73–116.

[6] W. Feller, *An Introduction to Probability Theory and Its Applications*, Vol. **1**, Third Edition, John Wiley, New York, 1968.

[7] M. I. Shamos, D. Hoey, Closest-point problems, in: Proceedings of the 16th Annual Symposium on Foundations of Computer Science, FOCS '75, IEEE Computer Society, Washington, DC, USA, 1975, pp. 151–162.

[8] D. Q. Naiman, H. P. Wynn, Inclusion-exclusion-Bonferroni identities and inequalities for discrete tube-like problems via Euler characteristics, *Annals of Statistics* **20** (1) (1992) 43–76.

[9] H. Edelsbrunner, The union of balls and its dual shape, *Discrete & Computational Geometry* **13** (1) (1995) 415–440.

[10] B. Chen, The incidence algebra of polyhedra over the Minkowski algebra, *Advances in Mathematics* **118** (2) (1996) 337 – 365.

[11] H. Edelsbrunner, Algebraic decomposition of non-convex polyhedra, in: Proc 36th Annual IEEE Symposium on Foundations of Computer Science, 1995, pp. 248–257.

[12] Maple 17, maplesoft, a division of Waterloo Maple Inc., Waterloo, Ontario.

[13] CGAL, Computational Geometry Algorithms Library, http://www.cgal.org.

[14] H. Edelsbrunner, P. Fu, Measuring space filling diagrams and voids, Tech. Rep. UIUC-BI-MB-94-01, Beckman Institute, Univ Illinois at Urbana-Champaign, Illinois (1994).

[15] M. de Berg, M. van Kreveld, M. Overmars, O. Schwarzkopf, *Computational Geometry: Algorithms and Applications*, Springer-Verlag New York, Inc., Secaucus, NJ, USA, 1997.

[16] H. Edelsbrunner, *Algorithms in Combinatorial Geometry*, Springer-Verlag New York, Inc., New York, NY, USA, 1987.

[17] J. Leray, Sur la forme des espaces topologiques et sur les points fixes des représentations, *Journal de Mathématiques Pures et Appliquées* **24** (1945) 95–167.

[18] K. Borsuk, On the imbedding of systems of compacta in simplicial complexes, *Fundamenta Mathematicae* **35** (1) (1948) 217–234.

[19] F. Aurenhammer, O. Schwarzkopf, A simple on-line randomized incremental algorithm for computing higher order voronoi diagrams, *International Journal of Computational Geometry & Applications* **2** (4) (1992) 363–381.

[20] C. Yap, T. Dubé, The exact computation paradigm, in: *Computing in Euclidean Geometry*, 2nd edition, eds D-Z Du and FK Hwang, World Scientific, 1995, pp. 452–486.